

band, this phenomenon does not have much practical significance.

If computation works sensibly, within the PBG frequency range, transmission and reflection should add up to unity in the 2D case. Thus, during the optimization process (for example), it suffices to study the transmission power only. Because reflection is not studied, short input WG can be used, which limits the computation space. Also, the post-processing time is halved, because only one observation plane is used. Assuming that one is only interested in the transmission of the bend structure shown in Figure 7, one could approximately halve the computation space and use a single observation plane. Then, in the 2D case, one optimization step (simulation plus post-processing) with 4000 FDTD time steps, 2×27 E-points, 27 H-points, takes about 100 sec using a PC with 700 MHz/770-MB RAM (the speed of field computation is 1000 time steps/18 sec).

5. CONCLUSION

Modelling PBG waveguide components has been considered, with field computation using FDTD. As an example, a 120° bend has been studied more closely, and power transmission results have been shown for various cases. The true necessity of bend geometry optimization has become apparent. Considering optimization, an approximative result for bend transmission is enough, that is, the spectrum does not have to fully converge. Then, with a 700-MHz PC, one optimization step (field computation and post-processing) takes a few minutes when using a 2-D model in field computation. Taking the finite-PBG plate thickness into account by using a 3D model will increase the needed time to tens of minutes.

With 2D bend structures, the convergence of the spectrum may be very slow in certain frequencies. With 3D structures this “ringing problem” is less severe, due to the radiation losses in the z direction. In general, the cell size $\Delta = a/10$ seems to be sufficient if studying these structures at frequencies $fa/c \leq 0.3$. This is an important point if one strives for quick optimization. However, there may be structures with special frequencies, which can be very sensitive to the cell size and the relative hole size d/a .

REFERENCES

1. F. Falcone et al., Novel photonic crystal waveguide in microwave printed-circuit technology, *Microwave Opt Technol Lett* 34 (2002), 462–466.
2. M. Qiu et al., Time-domain 2D modeling of slab-waveguide-based photonic-crystal devices in the presence of radiation losses, *Microwave Opt Technol Lett* 34 (2002), 387–393.
3. M. Lončar et al., Waveguiding in planar photonic crystals, *Appl Phys Lett* 77 (2000), 1937–1939.
4. M. Notomi et al., Extremely large group-velocity dispersion of line-defect waveguides in photonic crystal slabs, *Phys Rev Lett* 87 (2001), 253902.
5. M. Tokushima et al., Lightwave propagation through a 120° sharply bent single-line-defect photonic crystal waveguide, *Appl Phys Lett* 76 (2000), 952–954.
6. A. Taflov and S.C. Hagness, *Computational electrodynamics, the finite difference time domain method*, 2nd edition, Artech House, 2000.
7. K. Kärkkäinen, A. Sihvola and K. Nikoskinen, Analysis of a three-dimensional dielectric mixture with finite difference method, *IEEE Transactions on Geoscience and Remote Sensing* 39 (2001), 1013–1018.
8. T. Rozzi and M. Mongiardo, *Open electromagnetic waveguides*, IEE Electromagnetic wave series, vol. 43. The Institution of Electrical Engineers, London, UK, 1997.
9. A. Mekis et al., High transmission through sharp bends in photonic crystal waveguides, *Phys Rev Lett* 77 (1996), 3787–3790.
10. J.D. Joannopoulos, R.D. Meade, and J.N. Winn, *Photonic crystals, molding the flow of light*, Princeton University Press, Princeton, NJ, 1995.

© 2003 Wiley Periodicals, Inc.

Ka-BAND pHEMT MMIC VCO WITH WIDE TUNING RANGE

Seonghan Ryu,¹ Huijung Kim,¹ Jounghyun Yim,¹ Kyounghoon Im,² Youngwoong Kim,² Seogtae Han,³ and Bumman Kim¹

¹ Department of Electronic and Electrical Engineering
Microwave Application Research Center
Pohang University of Science and Technology
San 31, Hyoja Dong, Nam Gu
Pohang, 790-784, Korea

² Future Communications IC, Sungnam, Korea

³ Taeduk Radio Observatory, Taejeon, Korea

Received 14 April 2003

ABSTRACT: A Ka-band MMIC VCO utilizing 0.15- μm T-gate GaAs P-HEMT technology is presented. The VCO exhibits a low-phase noise property with wide tuning range of up to 3 GHz. A balanced buffer amplifier is also developed to ensure that the output power is higher than 10 dBm. The best measured phase noise at 1 MHz offset is -106 dBc/Hz. By varying the bias voltage of the on-chip varactor, the frequency can be continuously tuned from 33.3 to 36.3 GHz. In this frequency range, output power higher than 10 dBm has been measured without using the buffer amplifier. The buffer amplifier exhibits a typical gain of 5 dB with 15-dBm output power. A Lange coupler provides good matching between the VCO and the amplifier. © 2003 Wiley Periodicals, Inc. *Microwave Opt Technol Lett* 39: 333–336, 2003; Published online in Wiley InterScience (www.interscience.wiley.com). DOI 10.1002/mop.11206

Key words: wide tuning range; millimeter-wave VCO; P-HEMT technology

INTRODUCTION

As demand for higher-frequency systems such as high-speed optical communication networks and automotive radar systems has increased, millimeter-wave component technology has become very important. Tunable low-phase noise oscillators are key components in millimeter-wave systems. Several oscillators operating at millimeter-wave frequencies using HEMT or HBT technology have been reported [1–5]. Although HBT-based oscillators have exhibited better phase-noise performance than HEMT-based oscillators, the output power available from HBT-based oscillators cannot compete with that of HEMT-based oscillators. Also, the HBT process is not compatible with the P-HEMT process, which is the most favored millimeter-wave circuit technology. For high-level integration of monolithic VCOs with other MMIC components using the mature GaAs P-HEMT process at a low cost, VCOs based on P-HEMT technology are highly desired. The motivation of this work is to develop monolithic Ka-band VCOs with low phase noise, good power performance, and wide tuning range by utilizing conventional GaAs P-HEMT technology for full monolithic integration of a millimeter-wave transceiver. The P-HEMT-based Ka-band VCO which we have developed delivers a typical output power higher than 10 dBm at 35 GHz without a buffer amplifier. This VCO exhibits a tuning range of up to 3 GHz. The best measured phase noise at 1 MHz offset is -106 dBc/Hz.

CIRCUIT DESIGN

The oscillator's circuit topology is shown in Figure 1. A commercial 0.15- μm T-gate GaAs P-HEMT process of TRW foundry is used for the design. The active devices show a unity current gain cutoff frequency f_T of 81.1 GHz, maximum frequency of oscillation f_{MAX} of 110 GHz, and a pinchoff voltage of -0.9 V. A four-finger 120- μm P-HEMT device is chosen for output power

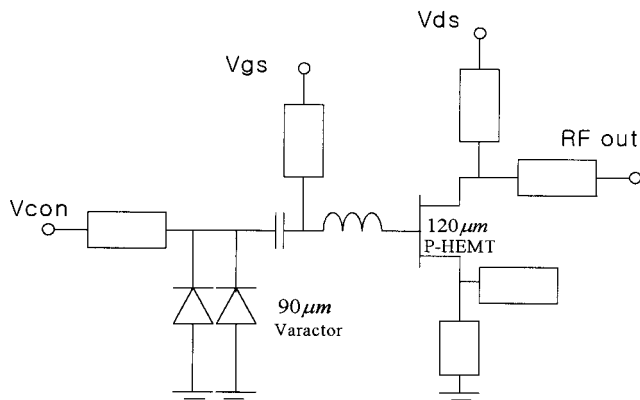


Figure 1 Circuit diagram of the VCO

higher than 10 dBm and two four-finger 90- μm varactors are connected in parallel and are attached to the VCO circuit in series with a main inductor for voltage-controlled operation with wide tuning range. The main inductor is implemented using a microstrip-line stub connected to the gate terminal of the active device. DC blocking capacitors to separate the RF-signal path from the varactors' and active devices' power supplies are implemented as MIM type and show a capacitance of 320 pF/mm². The bias point of this oscillator is chosen to maximize the output power. Therefore, the 120- μm P-HEMT is biased for Class A operation. The VCO design procedure follows the design example in [8]. The summation of reactances looking in and out from the gate terminal of a Q1 transistor is set to zero at the oscillation frequency of 35 GHz. To establish the required negative resistance at the drain terminal of the active device, two open microstrip-line stubs are connected to each side of the source terminal. After that, the load impedance is chosen for maximum output power. The design is performed using nonlinear harmonic balance simulation. All the microstrip line structures are modified utilizing an electromagnetic (EM) simulation to compensate the uncertainty of microstrip line model of the simulator at millimeter-wave band.

Figure 2 shows a chip photograph of the 35-GHz MMIC VCO. The VCO chip size is $2 \times 2.5 \text{ mm}^2$, and this size can be reduced further. The oscillator is fabricated on 100- μm substrate by TRW. The buffer amplifier is also designed to ensure that the output power is higher than 10 dBm. A balanced type of configuration, utilizing a Lange coupler, is used to minimize the load pulling of

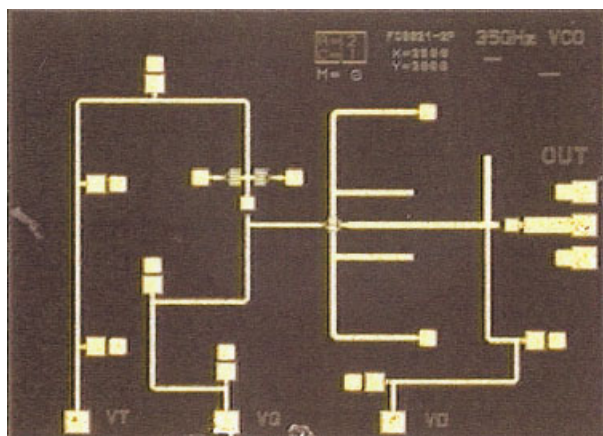


Figure 2 Photograph of the fabricated monolithic VCO [Color figure can be viewed in the online issue, which is available at www.interscience.wiley.com.]

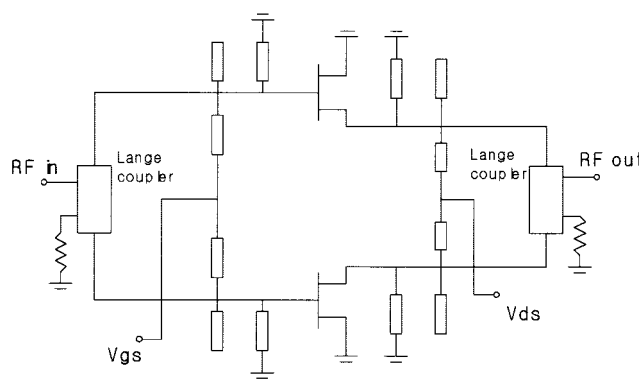


Figure 3 Circuit diagram of the buffer amplifier

the VCO. The buffer amplifier's schematic diagram is shown in Figure 3 and a chip photograph of the buffer amplifier is shown in Figure 4. A 120- μm P-HEMT device is used with the same bias point of the VCO. The chip size is $2 \times 2.5 \text{ mm}^2$.

MEASUREMENT RESULTS

The 35-GHz VCO and buffer amplifier are measured on wafer using RF probes, without any circuit tuning, using a 40-GHz spectrum analyzer. Figure 5 shows the setup used for measuring the frequency of oscillation and the output power of the VCO. Figure 6 shows the measurement results of the buffer amplifier. Input and output return loss is below -20 dB and gain is about 5 dB at 35 GHz. Figure 7 shows the measured and nonlinear simulated frequency tuning curve of the VCO, and Figure 8 displays the associated measured output power and RF to DC efficiency of the VCO connected with the buffer amplifier. Output power higher than 15 dBm is achieved over the total frequency tuning range from 33.3 to 36.3 GHz with a slight variation of power of less than 1 dB. The gain of the buffer amplifier is around 5 dB and the VCO generates output power of more than 10 dBm. The best measured phase noise of the VCO at 1 MHz offset is -106 dBc/Hz . The spectrum of the output power at a center frequency of about 35.5 GHz is shown in Figure 9. The total power consumption of the oscillator is about 60 mW at a supply voltage of 3 V. The RF-to-DC conversion efficiency is about 16% in the entire frequency tuning range. These performances are compared with the recently published results in Table 1. The output power of this

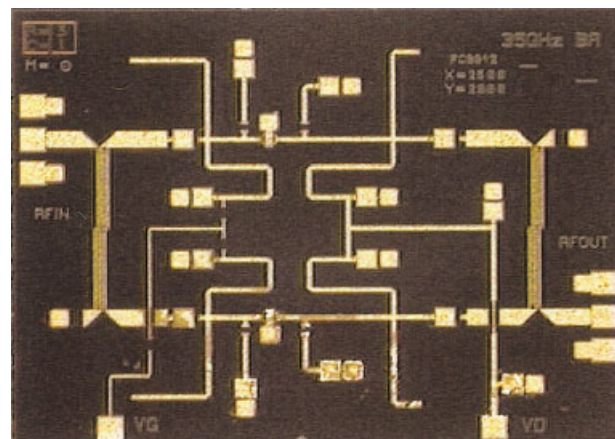


Figure 4 Photograph of the buffer amplifier [Color figure can be viewed in the online issue, which is available at www.interscience.wiley.com.]

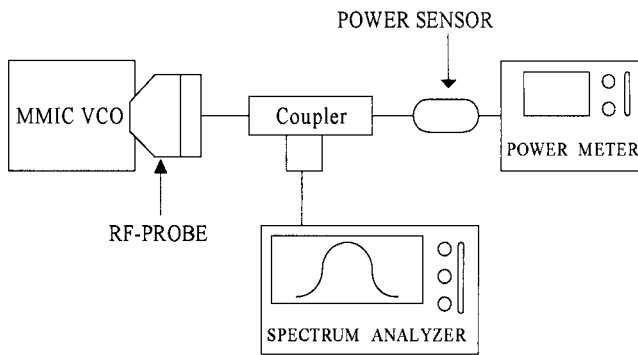


Figure 5 Test setup for measuring frequency of oscillation and output power

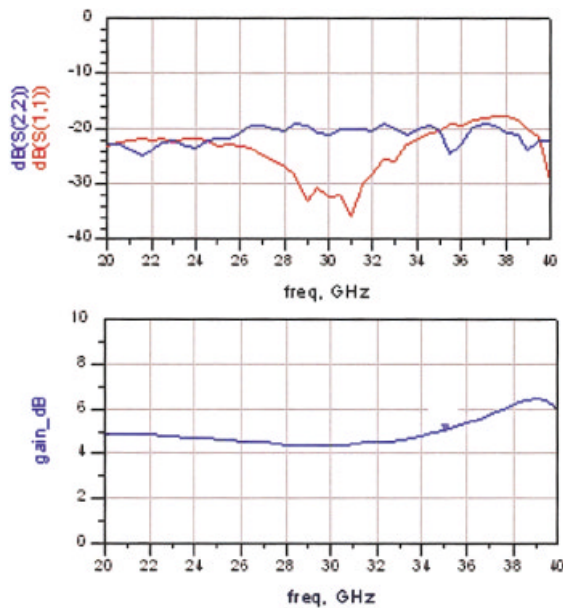


Figure 6 Measured return loss (above) and gain (below) of the buffer amplifier [Color figure can be viewed in the online issue, which is available at www.interscience.wiley.com.]

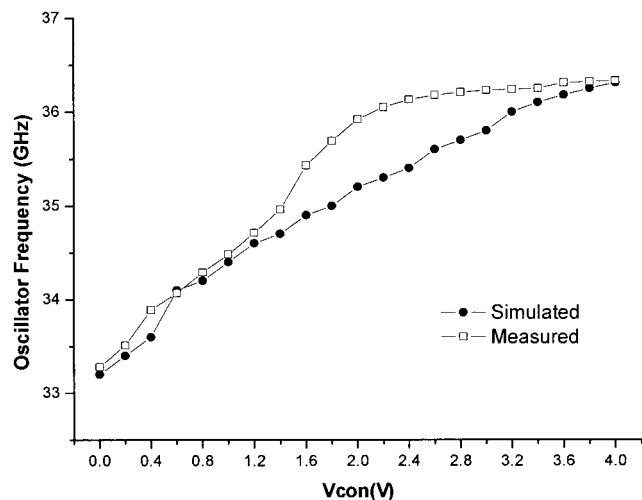


Figure 7 Measured and nonlinear simulated frequency tuning with applied control voltage of the 35-GHz VCO with buffer amplifier

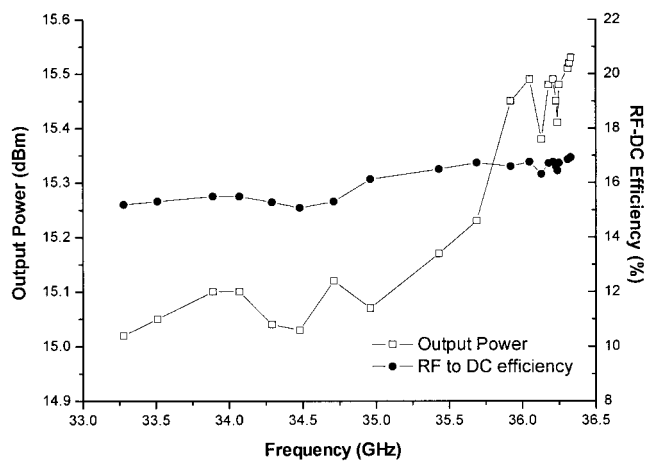


Figure 8 Measured output power and RF-to-DC efficiency of the VCO with buffer amplifier

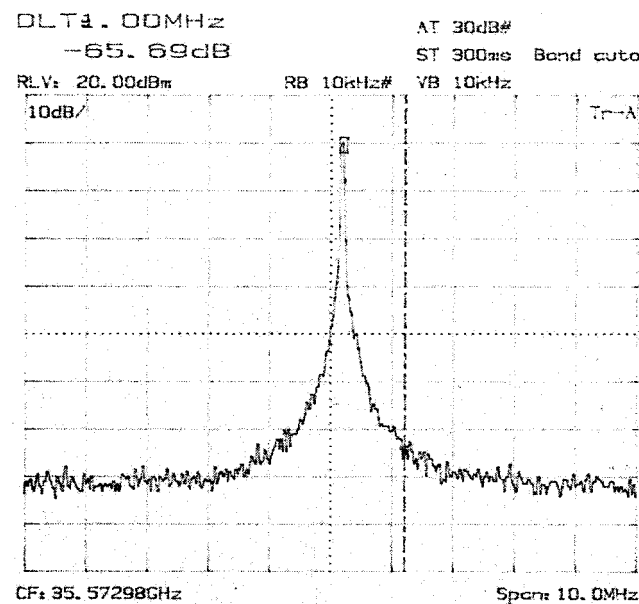


Figure 9 Output spectrum of the 35-GHz VCO

VCO is higher than that of HBT-based VCOs with comparable phase noise.

CONCLUSION

In this paper, a 35-GHz P-HEMT-based MMIC VCO is presented. It uses 0.15- μm T-gate GaAs P-HEMT device technology. All the microstrip line structures are modified utilizing an EM simulation. The VCO has exhibited a frequency tuning range of up to 3 GHz and output power higher than 10 dBm. The best measured phase noise at 1-MHz offset is -106 dBc/Hz. When it is amplified by the buffer amplifier, the power level is increased to 15 dBm. The low-phase noise, wide tuning range, and good output power performance of the VCO enable a high-level and cost-effective integration of multifunctional MMICs at the millimeter-wave band for various applications such as single-chip transceivers in wireless communication systems or automotive radar systems.

ACKNOWLEDGMENTS

This work was supported by the Agency for Defense Development and Brain Korea 21 projects of the ministry of education in Korea.

TABLE 1 Comparison of Performances of Previously Published Oscillators at the Millimeter-Wave Band

	Process	Oscillation Frequency (GHz)	Output Power (dBm)	Phase Noise at 1-MHz offset (dBc/Hz)	Tuning Range (GHz)
This work	P-HEMT	35	10	-106	3
Kurdoghlian [1]	AlGaAs/InGaAs HBT	39	2	-95	3.5
Wang [3]	P-HEMT	90.5	8.8	-68.2	0.6
Riepe [4]	GaN/InP/GaAs HBT	35	<3.5	-107	1

REFERENCES

1. A. Kurdoghlian et al., 40-GHz fully integrated and differential monolithic VCO with wide tuning range in AlInAs/InGaAs HBT, 23th Ann IEEE GaAs IC Symp Dig, 2001, pp. 129–131.
2. Y. Kwon et al., Large signal analysis and experimental characteristics of monolithic InP-base W-band HEMT oscillators, 21th Euro Microwave Conf Tech Dig, Stuttgart, Germany, 1991.
3. H. Wang et al., Monolithic W-band VCOs using pseudomorphic AlGaAs/InGaAs/GaAs HEMT's, 14th Ann IEEE GaAs IC Symp Dig, Philadelphia, PA, 1994, pp. 30–33.
4. K. Riepe et al., 35–40-GHz Monolithic VCOs utilizing high speed GaInP/GaAs HBT's, IEEE Microwave Guided Wave Lett 4 (1994), 274–276.
5. S.H. Ryu et al., Monolithic Ka-band VCO with wide tuning range, 32nd Euro Microwave Conf Dig, Milan, Italy, 2002, pp. 845–847.
6. H. Wang et al., An ultra low noise monolithic three stage amplifier using 0.1 μm InGaAs/GaAs pseudomorphic HEMT technology, 1992 IEEE MTT-S Int Microwave Symp Dig, New Mexico, 1992, pp. 803–806.
7. K.W. Chang et al., A W-band monolithic down converter, IEEE Trans Microwave Theory Tech MTT-39 (1991), 1972–1979.
8. G. Gonzales, Microwave transistor amplifier analysis and design, Prentice-Hall, Englewood Cliffs, NJ, 1998, Ch. 5.

© 2003 Wiley Periodicals, Inc.

A NEW RELATION BETWEEN POLARIZATION-MODE DISPERSION VECTOR AND OUTPUT STATE OF POLARIZATION

G. X. Ning,¹ S. Aditya,¹ P. Shum,¹ C. Q. Wu,² and Y. D. Gong³

¹ Network Technology Research Center (S2-B3c-23)
Nanyang Technological University
Nanyang Avenue
Singapore 639798

² Northern Jiaotong University
Beijing, China 100044

³ Institute for InfoComm Research
Innovation Center Block 2
Nanyang Drive
Singapore 637723

Received 30 April 2003

ABSTRACT: We derive a new relation to show that, as frequency changes, the output state of polarization vector precesses around the PMD vector with a fixed angle of precession. The new relation leads to a familiar expression for pulse broadening. Based on this expression, a PMD compensator is suggested and measured results are given for a 10-Gb/s signal. © 2003 Wiley Periodicals, Inc. Microwave Opt Technol Lett 39: 336–338, 2003; Published online in Wiley InterScience (www.interscience.wiley.com). DOI 10.1002/mop.11207

Key words: PMD; pulse broadening due to PMD; PMD compensation

INTRODUCTION

Polarization-mode dispersion (PMD) can cause severe limitations in fiber-optical communication systems. Polarization-mode dispersion is characterized by the PMD-vector, $\vec{\Omega}$, in the Stokes space, around which an output state of polarization (SOP), $\vec{S}_o(\omega)$, precesses when the carrier frequency is changed [1]:

$$\frac{\partial \vec{S}_o}{\partial \omega} = \vec{\Omega} \times \vec{S}_o(\omega). \tag{1}$$

The modulus of the PMD vector, $\Delta\tau = |\Omega|$, is referred to as the different group delay (DGD); the DGD is the time delay between the two principal states of polarization (PSPs), $\hat{e}_{\Omega\pm}$, which are the two eigen-polarizations. A well-known manifestation of PMD is pulse broadening. To reduce this pulse-broadening, a number of PMD-compensation techniques have been proposed in the literature [2–5]. In this paper, we derive a new analytical expression that relates the frequency-dependent output state of polarization and the PMD vector. Only the first-order PMD is considered here. The interpretation of this relation is consistent with the established behavior of $\vec{S}_o(\omega)$ with respect to $\vec{\Omega}$. Following this, we also give a new derivation for an analytical expression for the RMS pulsewidth σ for a Gaussian pulse affected by the first-order PMD. The concept of RMS pulsewidth in the context of PMD was introduced in [6, 7]. This method of calculation does not use the Taylor expansion. From the expression for σ , we can know how to compensate the PMD. Accordingly, a PMD compensator scheme, based on nullifying DGD, is implemented and measured results for a 10-Gb/s signal are reported.

RELATION BETWEEN OUTPUT POLARIZATION STATE AND PMD VECTOR

We begin with Eq. (1), which connects the PMD vector $\vec{\Omega}$, $\vec{\Omega} = [\Omega_1, \Omega_2, \Omega_3]^T$, and output state of polarization $\vec{S}_o(\omega) \cdot \vec{\Omega} \times$ can be interpreted as a skewsymmetric matrix P corresponding to the cross-product operator. The matrix P is given by

$$\vec{\Omega} \times = P = \begin{bmatrix} 0 & -\Omega_3 & \Omega_2 \\ \Omega_3 & 0 & -\Omega_1 \\ -\Omega_2 & \Omega_1 & 0 \end{bmatrix}. \tag{2}$$

Then Eq. (1) can be rewritten as

$$\frac{\partial \hat{S}_o(\omega)}{\partial \omega} = P \hat{S}_o(\omega), \tag{3}$$

where $\hat{S}_o(\omega)$ is a unit vector in the direction of the output state of polarization. When we do not take higher-order PMD into account, the PMD vector and the matrix P can be considered to be constant. The solution of Eq. (3) can then be given by

$$\hat{S}_o = \exp\{P(\omega - \omega_0)\} \hat{S}_o(\omega_0), \tag{4}$$